The Structures and Stabilities of the Complexes of Biologically Available Ligands with Fe(III)–Porphine: An Ab Initio Study

ARTICLE *in* THE JOURNAL OF PHYSICAL CHEMISTRY B · JANUARY 2011

Impact Factor: 3.3 · DOI: 10.1021/jp1090747 · Source: PubMed

THE JOURNAL OF PHYSICAL CHEMISTRY B

Article

pubs.acs.org/JPCB

The Structures and Stabilities of the Complexes of Biologically Available Ligands with Fe(II) Porphine: An Ab Initio Study

Tebikie Wondimagegn and Arvi Rauk*

Department of Chemistry, University of Calgary, Calgary, Alberta, Canada T2N 1N4

Supporting Information

ABSTRACT: Fe(II) porphine complexes were investigated at the "MP2/LB"//B3LYP/SB level of theory where SB and LB denote the small and large basis sets, 6-31+G(d) and 6-311+G(2df,2p), respectively. Solvation effects due to water and benzene were approximated by the IEFPCM procedure. Ligands included H_2O, Cl^-, and OH^- and Im (imidazole), CH_3NH_2, $(CH_3)_2S$, $CH_3CO_2^-$, CH_3S^-, and CH_3PhO^- as models of the side chains of His, Lys, Met, Asp/Glu, Cys, and Tyr residues, respectively. Fe(II) porphine, **2**, and the complexes **2**(H_2O), **2**(Im), **2**$(CH_3)_2S$), **2**(CH_3NH_2), and **2**$(H_2O)_2$ have triplet ground states. All pentacoordinated complexes of **2** with negatively charged ligands have high spin quintet ground states, while all hexacoodinated complexes with at least one Im ligand have low spin singlet ground states. With the exception of **2**$(Im)_2$ and **2**(Im)$((CH_3)_2S)$, no hexacoordinated complexes are stable in water or benzene. Redox properties are sensitive to the nature of the environment and the ligand(s) attached to the iron center. With the exception of the parent system, $\mathbf{2}^+/\mathbf{2}$, all complexes are predicted to have a negative reduction potential relative to the standard hydrogen electrode in water. With neutral ligand(s), the reduction potential is higher in the nonpolar environment. The opposite is true with negatively charged ligands. The redox activity of cytochromes, peroxidases, and catalases is discussed in the context of the model parent systems.

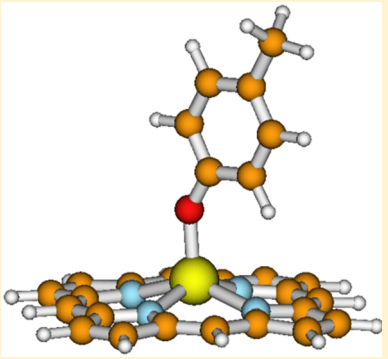

INTRODUCTION

Iron porphyrins play a vital role in biochemical processes, notably in the form of the prosthetic group, heme in hemoproteins. The processes include oxygen transport in animals (hemoglobin, myoglobin, neuroglobin, hemocyanin) and plants (leghemoglobin) and redox processes such as electron transfer (cytochrome c, catalase) and oxidative catalysis (peroxidases).

Heme, **1**, is a complex between iron and protoporphyrin IX. In nature, heme may be covalently linked to its enzyme, as in some cytochrome P450 (CYP4) enzymes,[1] or more frequently, it may be attached via a cysteine−iron bond (also in the CYP4 family),[2] a histidine−iron bond (e.g., myoglobin[3] or cytochrome c[4,5]), or a tyrosine−iron bond (catalase).[6]

Our principal interest lies in the fact that heme associates with the beta amyloid peptide (Aβ) of Alzheimer's disease, and that the complex has been shown to have peroxidase activity.[7] Beyond the discovery that Aβ seems to have two binding sites for heme, in the hydrophilic domain, residues 1−16, and in the hydrophobic domain, residues 17−40/42, and that heme and Cu(II) appear to bind independently of each other,[8] little is known about the nature of binding.[9] Aβ lacks Cys residues so the attachment cannot be of the cytochrome P450 kind. Aβ has a Tyr residue so the binding could be of the catalase kind. However, the peroxidase-like activity argues against this, and suggests that the heme could be attached to one of the three His residues, at positions 6, 13, and 14, all of which are exposed to the aqueous medium and serve as binding sites for Cu(II).

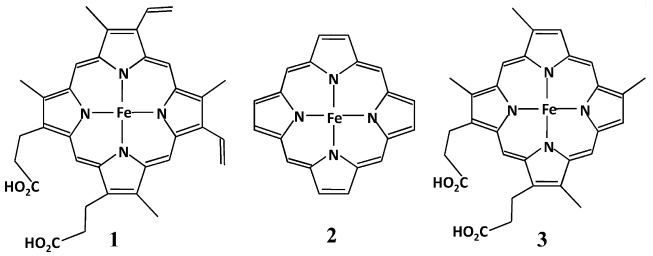

Virtually everything that is known about the parent systems, **2** (we will use an unsuperscripted number, e.g., **1**, to denote the neutral Fe(II) porphyrin complexes, and, e.g., $\mathbf{1}^+$, to denote the oxidized Fe(III) porphyrin complexes) and $\mathbf{2}^+$, is from theoretical calculations of which there are many.[10−18] Because **2**, the simplest system, is rather large, with 37 atoms, including a transition metal of uncertain spin state, and 184 electrons, it was not possible to do high-level calculations until the early 1990s when CI methods and density functional methods, combined with faster computers, could be applied to the task. It is now known with fair certainty from computations that the structure of **2** has D_{4h} symmetry. The ground state is most probably an intermediate spin triplet with several electronic configurations lying within a few kJ mol^{-1} of each other. Most computational models yield ^3E_g as the ground state, with the $^3A_{2g}$ state lying within about 4 kJ mol^{-1}, and several quintet

Received: June 14, 2012
Revised: August 3, 2012
Published: August 8, 2012

states just a few kJ mol^{-1} higher still.[12] The Fe(II)−N bond distance is 2.00 Å.[12]

Despite the numerous theoretical studies on **2** and other porphyrins, including complexes with various ligands, we can find only one that addressed the question of binding affinities, that for O_2, CO, and NO.[19] Experimental data on this question are plentiful.[20−22] Good binding affinity data exist for some hemochromes, which are hexacoordinated Fe(II) porphyrins with two nitrogen bases. In general, the affinity of Fe(II) porphyrins for imidazoles is about 1.0×10^2 M^{-1}.[20] Deuteroheme **3** binds two imidazoles successively in benzene with affinity constants $K_1 = 4.5 \times 10^3$ M^{-1} and $K_2 = 6.8 \times 10^4$ M^{-1}.[23]

$$\mathbf{3} + \mathrm{Im} \rightleftarrows \mathbf{3}(\mathrm{Im}) \qquad K_1,\ \Delta G_1,\ \Delta H_1 \tag{1}$$

$$\mathbf{3}(\mathrm{Im}) + \mathrm{Im} \rightleftarrows \mathbf{3}(\mathrm{Im})_2 \quad K_2,\ \Delta G_2,\ \Delta H_2 \tag{2}$$

Similarly, in benzene at 25 °C, the binding constants of pyridine to Fe(II) tetraphenylporphyrin have been estimated at $K_1 = 1.5 \times 10^3$ M^{-1} and $K_2 = 1.9 \times 10^4$ M^{-1}.[24] The atypical occurrence of K_2 being greater than K_1 in successive equilibria is the reason **1**(Im) dissociates into **1** and **1**$(Im)_2$.[25] The procedures described below have been shown to yield good agreement with the experimental data for **3**: exptl, $\Delta G_1 = -21$ kJ mol^{-1}, $\Delta G_2 = -28$ kJ mol^{-1} in benzene at 298 K; calc, $\Delta G_1 = -29$ kJ mol^{-1}, $\Delta G_2 = -43$ kJ mol^{-1}.[18]

Preparatory to a detailed investigation of the Aβ−heme interaction and its chemistry, we initiated a computational examination the binding possibilities for heme, as modeled by the parent system, iron porphine **2** and $\mathbf{2}^+$. The preliminary study focused mainly on the Fe(III) system, $\mathbf{2}^+$, with various biologically available ligands: H_2O, CH_3S^- (i.e., Cys), imidazole (Im, i.e., His), 4-CH_3PHO^- (i.e., Tyr), CH_3NH_2 (i.e., Lys, N-terminus), $CH_3CO_2^-$ (i.e., Asp, Glu, C-terminus), and $(CH_3)_2S$ (i.e., Met). All 5- and a number of 6-coordinate complexes were considered.[18] In the present work, we address the analogous Fe(II) species and calculate redox properties. Many heme reduction potentials have been measured over the last half century and are found to vary over a wide range. For instance, among peroxidases, values range from about 0 V versus SHE (versatile peroxidase) to −0.3 V (horse radish peroxidase).[26,27] The reasons for the variability are not well understood and will be discussed below in connection with the computed results.

COMPUTATIONAL METHODS

Density functional theory (DFT) and some Moller−Plesset second order (MP2) calculations were carried out using the Gaussian 03[28] and Gaussian 09[29] programs. All geometry optimizations and vibrational frequency analyses were performed using the Becke three-parameter hybrid functional (B3LYP) method[30] with the small basis set (SB), where SB = 6-31+G(d). B3LYP has been found to perform satisfactorily for predicting the spin states of iron porphines.[14] We note here that MP2 calculations are unreliable to predict the relative energies of the spin states. Thus, the B3LYP procedure was used as the basis for selecting the lowest spin state. The MP2 procedure almost always yielded a higher energy wave function for a given spin state, or the UHF step failed to converge. However, use of the B3LYP wave function as a guess for the UHF wave function and then the MP2 procedure invariably gave the lowest energy result for the same multiplicity. After each geometry optimization, single-point calculations have been carried out at the B3LYP/LB level of theory, where LB = 6-311+G(2df,2p), to obtain more accurate enthalpy changes. A scale factor of 0.9806 was used to scale the zero-point energies.[31] Unscaled frequencies were used to derive entropies and thermal corrections to the enthalpy. The entropy of each of the species was reduced by 26.58 J mol^{-1} K^{-1} ($=R\ln(1/24.465)$) to account for the change of state from gas at 1 atm pressure to 1 M solution. For all of the systems, enthalpies used to calculate binding affinities were derived at the "MP2/LB" level of theory, where E("MP2/LB") ≈ E(MP2/SB) + E(B3LYP/LB) − E(B3LYP/SB).[18,32,33] We are aware that MP2 results are subject to rather large basis set superposition errors (BSSEs).[34,35] However, it was not possible to calculate counterpoise corrections for any of the present porphine systems because intermediate calculations converged to higher states or failed to converge.

The polarizable continuum model (PCM) using the integral equation formalism variant (IEFPCM)[36] applied to the B3LYP/6-31+G(d) wave function was used to calculate the free energy of solvation in water and benzene. In the default procedure in G03, united atom Hartree−Fock (UAHF) radii are scaled by the factor 1.2. For the small *neutral* molecules considered here, this procedure yields absolute free energies of solvation in very good agreement with experimental values (ΔG_{solv}(calc), ΔG_{solv}(exptl),[37] in kJ mol^{-1}: H_2O, −30, −26; CH_3CO_2H, −30, −28; CH_3PhOH, −28, −28 (phenol); CH_3NH_2, −22, −19 (ethylamine); CH_3SH, −6, −5; $(CH_3)_2S$, −5, −6). On the other hand, we find that this procedure seriously underestimates the free energy of solvation of *charged* species and leads to calculated pK_a values that are up to 6 units higher than experimental values. While part of the error may reside in the calculated enthalpy differences, we assume that the entire error resides in the calculated ΔG_{solv} of the ionic species. Values of ΔG_{solv} for the small ionic species, were adjusted to give the correct experimental pK_a values assuming the calculated values for the neutral conjugate acids/bases are correct. Values used in this paper to calculate free energy changes in aqueous solution are (ΔG_{solv}, in kJ mol^{-1}): OH^-, −433; $CH_3CO_2^-$, −316; $CH_3NH_3^+$, −316; CH_3PhO^-, −300; CH_3S^-, −313; Cl^-, −322. In most cases, these are close to listed experimental values (ΔG_{solv}(exptl),[37] in kJ mol^{-1}): OH^-, −444; $CH_3CO_2^-$, −322; $CH_3NH_3^+$, −293; Cl^-, −322 (it should be noted that, for the ions, there are large uncertainties in the experimental values of ΔG_{solv}). Experimental free energies of solvation have been used for H_2O (ΔG_{solv} = −26.4 kJ mol^{-1})[38] and H^+ (ΔG_{solv} = −1107 kJ mol^{-1}).[39] An addition of 10 kJ mol^{-1} ($=RT\ln(55.6)$ kJ mol^{-1}) was made to the free energy of solvation of water when water itself is the solvent, since liquid water is 55.6 M.

For iron porphines, **2** and $\mathbf{2}^+$, and their complexes, the default factor of 1.2 was used for all species.

The solvation free energies have also been calculated in benzene, a solvent with a low dielectric constant ($\varepsilon = 2.27$), to mimic the protein environment where the effective dielectric constant ranges from 2 to 16[40] and, in some cases, to enable comparison with experimental results.

As well as the parent **2**, we have studied five- and six-coordinate complexes. Singlet, triplet, and quintet states have been considered. All the calculations were carried out using the spin-unrestricted formalism for open shell systems.

Standard reduction potentials, $E°$("Fe^{3+}"/"Fe^{2+}") vs the standard hydrogen electrode (SHE), were calculated from the half reactions

Table 1. Optimized Structural Parameters (Å) of Fe(II) Porphines at the B3LYP/6-31+G(d) Level

			bond distances				
complex[a]	spin state	out-of-plane displacement[b]	Fe−N_{por}[c]	Fe−N_{lig}	Fe−O	Fe−S	Fe−Cl
2	triplet		2.003				
2(Im)	triplet	0.15	2.020	2.258			
2$(CH_3)_2S$)	triplet	0.08	2.012	2.997			
2($MePhO^-$)$^-$	quintet	0.41	2.155		1.939		
2(OAc^-)	quintet	0.61	2.151		1.975		
2(CH_3S^-)	quintet	0.64	2.160			2.384	
2(CH_3NH_2)	triplet	0.13	2.018	2.302			
2(H_2O)	triplet	0.07	2.016		2.427		
2(OH^-)	quintet	0.67	2.095		1.908		
2(Cl^-)	quintet	0.50	2.095				2.225
2$(H_2O)_2$	triplet	0.00	2.012		2.520/2.525		
2$(Im)_2$	singlet	0.00	2.022	2.034			
2(Im)(Cl^-)	singlet	0.01	2.023	2.042			2.399
2(Im)(OAc^-)	singlet	0.01	2.024	2.042	1.994		
2(Im)(CH_3S^-)	singlet	0.03	2.021	2.116		2.377	
2(Im)($MePhO^-$)	singlet	0.02	2.022	2.044	1.995		
2(Im)(($CH_3)_2S$)	singlet	0.01	2.023	2.029		2.414	
$\mathbf{2}^+$(Im)(Cl^-)	doublet	0.19	2.024	2.547			2.329
$\mathbf{2}^+$(Im)(OAc^-)	quartet	0.21	2.028	2.525	1.964		
$\mathbf{2}^+$(Im)(($CH_3)_2S$)	hextet	0.01	2.004	2.227		2.903	

[a]See Figures 1 and 2. [b]Fe displacement from the mean porphine nitrogen plane. [c]Average Fe−$N_{porphine}$ distances.

Table 2. Selected Reactions of Penta- and Hexacoordinated Complexes of 2 and 2^+ (All Units Are in kJ mol^{-1})

reaction	$\Delta H_{(g)}$(0K)	$\Delta H_{(g)}$(298K)	$-T\Delta S$	$\Delta G_{(g)}$	$\Delta\Delta G_{solv}$	$\Delta G_{(aq)}$	pK_a	$\Delta\Delta G_{solv}$	$\Delta G_{(bz)}$
2 + H_2O → **2**(H_2O)	−36.8	−37.3	23.2	−14.1	13.6	−0.5		12.2	−1.9
2 + $(CH_3)_2S$ → **2**(($CH_3)_2S$)	−74.9	−72.1	28.1	−44.0	37.7	−6.3		37.2	−6.8
2 + Im → **2**(Im)	−91.2	−88.6	30.8	−57.9	42.2	−15.7		29.0	−28.9
2 + CH_3NH_2 → **2**(CH_3NH_2)	−70.9	−72.5	39.4	−33.1	33.3	0.2		14.7	−18.6
2 + OAc^- → **2**(OAc^-)	−217.6	−216.1	34.5	−181.6	162.2	−19.4		100.6	−81.0
2 + Cl^- → **2**(Cl^-)	−248.1	−246.6	12.8	−233.8	157.3	−76.5			
2 + $MePhO^-$ → **2**($MePhO^-$)	−273.9	−269.7	26.0	−243.7	165.1	−78.7		83.6	−160.2
2 + CH_3S^- → **2**(CH_3S^-)	−289.3	−285.6	23.6	−261.9	162.7	−99.2		87.6	−174.3
2 + OH^- → **2**(OH^-)	−299.7	−299.1	16.9	−282.2	249.2	−33.0			
2 + $CH_3NH_3^+$ → **2**(CH_3NH_2) + H^+	819.6	824.1	13.0	837.1	−780.0	57.0	10		
2 + MePhOH → **2**($MePhO^-$) + H^+	1174.4	1184.1	2.2	1186.3	−1213.9	−27.6	−5		
2 + CH_3SH → **2**(CH_3S^-) + H^+	1199.4	1208.0	2.1	1210.1	−1251.4	−41.3	−7		
2 + H_2O → **2**(OH^-) + H^+	1354.0	1360.1	−25.9	1334.2	−1288.0	46.2	8		
2(H_2O) + H_2O → **2**$(H_2O)_2$	−31.8	−31.1	24.0	−7.1	17.4	10.3		22.2	15.1
2(Im) + Im → **2**$(Im)_2$	−124.1	−125.9	58.1	−67.7	42.7	−25.0		24.7	−43.0
2(Im) + $(CH_3)_2S$ → **2**(Im)(($CH_3)_2S$)	−117.0	−118.5	55.5	−62.9	36.6	−26.4		34.0	−28.9
2(Im) + OAc^- → **2**(Im)(OAc^-)	−110.3	−110.9	51.4	−59.2	154.1	94.6		109.6	50.1
2(Im) + Cl^- → **2**(Im)(Cl^-)	−98.1	−100.8	36.5	−64.3	130.6	66.3		101.1	36.8
2(Im) + $MePhO^-$ → **2**(Im)($MePhO^-$)	−124.3	−124.2	47.0	−77.2	160.2	83.0		77.9	0.8
2(Im) + CH_3S^- → **2**(Im)(CH_3S^-)	−144.0	−147.0	55.8	−91.2	144.9	53.7		76.5	−14.7
2(CH_3S^-) + Im → **2**(Im)(CH_3S^-)	54.2	49.9	62.9	112.9	24.4	137.2		17.9	130.7
$\mathbf{2}^+$(Im) + $(CH_3)_2S$ → $\mathbf{2}^+$(Im)(($CH_3)_2S$)	−103.4	−100.6	33.7	−66.9	40.1	−26.9		−21.3	−88.2
$\mathbf{2}^+$(Im) + Cl^- → $\mathbf{2}^+$(Im)(Cl^-)	−418.7	−420.9	28.3	−392.6	416.9	24.3		251.6	−140.9

$$\text{“}Fe^{3+}\text{”}_{(aq)} + e^- \rightarrow \text{“}Fe^{2+}\text{”}_{(aq)} + aL \qquad \Delta G^{Fe} \tag{3}$$

and

$$H^+ + e^- \rightarrow {}^1/_2H_2 \qquad \Delta G^{SHE} \tag{4}$$

where “Fe^{3+}” and “Fe^{2+}” represent all of the oxidized and reduced iron species involved in the reduction and ΔG^{Fe} and ΔG^{SHE} are the aqueous free energy changes for the respective half reactions, ignoring the electron. The symbol *a*L recognizes the fact that a number of ligands may be shed in the reduction process, and the associated entropy change may be an important component of the free energy change. Thus,

$$E^\circ(\text{“}Fe^{3+}\text{”}/\text{“}Fe^{2+}\text{”}) = -(\Delta G^{Fe} - \Delta G^{SHE})/F \tag{5}$$

where F is the Faraday constant, F = 96.485 kJ mol^{-1} V^{-1}. For the reduction of the proton, we adopt the experimental value ΔG^{SHE} = −418 kJ mol^{-1}.[41] The actual potential, E, of the half reaction under ambient conditions is related to the standard potential, E°, through the Nernst equation:

dx.doi.org/10.1021/jp305864y | J. Phys. Chem. B 2012, 116, 10301−10310

Table 3. Reduction Reaction Energetics and Reduction Potentials in Water and Benzene (V vs SHE)

reduction reaction	$\Delta H_{(g)}$(298K)	$-T\Delta S$	$\Delta G_{(g)}$	$\Delta\Delta G_{solv}$	$\Delta G_{(aq)}$	$E^{\circ}_{(aq)}$	$\Delta\Delta G_{solv}$	$\Delta G_{(bz)}$	$E^{\circ}_{(bz)}$
$\mathbf{2}^+ + e^- \rightarrow \mathbf{2}$	−603.1	3.1	−600.0	137.2	−462.9	0.47	79.5	520.5	1.06
$\mathbf{2}^+(Cl^-) + e^- \rightarrow \mathbf{2}(Cl^-)$	−235.9	−3.4	−239.3	−169.6	−408.9	−0.09	−87.1	−326.4	−0.95
$\mathbf{2}^+(OH^-) + e^- \rightarrow \mathbf{2}(OH^-)$	−107.7	−4.1	−111.8	−174.3	−286.1	−1.37	−83.8	−195.6	−2.31
$\mathbf{2}^+(OH^-) + H^+ + Cl^- + e^- \rightarrow \mathbf{2}(Cl^-) + H_2O$	−1677.1	11.4	−1665.7	1257.3	−408.3	−0.51[a]	−90.6[b]	−429.1[b]	0.12[b]
$\mathbf{2}^+(OH^-) + H^+ + OAc^- + e^- \rightarrow \mathbf{2}(OAc^-) + H_2O$	−1646.5	33.1	−1613.4	1262.3	−351.2	−1.11[a]	−59.8[c]	−263.2[c]	−1.60[c]
$\mathbf{2}^+(OH^-) + H^+ + Im + e^- \rightarrow \mathbf{2}(Im) + H_2O$	−1519.1	29.3	−1489.7	1142.2	−347.5	−1.15[a]	120.2[d]	−458.2[d]	0.42[d]
$\mathbf{2}^+(OH^-) + CH_3SH + e^- \rightarrow \mathbf{2}(CH_3S^-) + H_2O$	−222.4	0.7	−221.7	−151.4	−373.1	−0.46	−77.5	−299.3	−1.23
$\mathbf{2}^+(OH^-) + MePhOH + e^- \rightarrow \mathbf{2}(MePhO^-) + H_2O$	−246.3	0.8	−245.5	−113.9	−359.4	−0.61	−59.4	−304.9	−1.17
$\mathbf{2}^+((CH_3)_2S) + e^- \rightarrow \mathbf{2}((CH_3)_2S)$	−531.4	−1.5	−533.0	123.4	−409.5	−0.09	73.3	−459.6	0.43
$\mathbf{2}^+(Im) + e^- \rightarrow \mathbf{2}(Im)$	−499.0	−1.8	−500.8	115.4	−385.4	−0.34	72.9	−429.7	0.10
$\mathbf{2}^+(OAc^-) + e^- \rightarrow \mathbf{2}(OAc^-)$	−167.2	3.5	−163.8	−161.8	−325.6	−0.96	−64.3	−228.1	−1.97
$\mathbf{2}^+(CH_3NH_2) + e^- \rightarrow \mathbf{2}(CH_3NH_2)$	−521.4	7.3	−514.1	139.1	−375.0	−0.45	79.8	−434.3	0.17
$\mathbf{2}^+(MePhO^-) + e^- \rightarrow \mathbf{2}(MePhO^-)$	−201.6	−2.6	−204.1	−154.2	−358.3	−0.62	−72.4	−276.5	−1.47
$\mathbf{2}^+(CH_3S^-) + e^- \rightarrow \mathbf{2}(CH_3S^-)$	−189.8	−3.7	−193.4	−165.7	−359.1	−0.61	−82.7	−276.1	−1.47
$\mathbf{2}^+(Im)_2 + e^- \rightarrow \mathbf{2}(Im)_2$	−498.2	1.2	−497.0	111.8	−385.2	−0.34	67.4	−429.6	0.12
$\mathbf{2}^+(Im)((CH_3)_2S) + e^- \rightarrow \mathbf{2}(Im)((CH_3)_2S)$	−516.8	20.0	496.8	111.9	−384.9	−0.34	57.4	−439.4	0.22
$\mathbf{2}^+(Im)(Cl^-) + e^- \rightarrow \mathbf{2}(Im)(Cl^-)$	−178.8	6.3	−172.6	−170.9	−343.4	−0.77	−77.6	−250.2	−1.74
$\mathbf{2}^+(Im)(OAc^-) + e^- \rightarrow \mathbf{2}(Im)(OAc^-)$	−168.7	15.7	−153.0	−165.4	−318.4	−1.03	−82.6	−235.6	−1.89
$\mathbf{2}^+(Im)(MePhO^-) + e^- \rightarrow \mathbf{2}(Im)(MePhO^-)$	−178.4	−14.0	−192.4	−150.0	−342.3	−0.78	−72.1	−264.5	−1.59
$\mathbf{2}^+(Im)(CH_3S^-) + e^- \rightarrow \mathbf{2}(Im)(CH_3S^-)$	−123.1	5.9	−117.2	−168.3	−285.5	−1.37	−81.3	−198.5	−2.27
$\mathbf{2}^+(Im)(H_2O) + e^- \rightarrow \mathbf{2}(Im) + H_2O$	−441.9	−27.5	−469.5	106.9	−362.6	−0.57	54.3	−415.2	−0.03
$\mathbf{2}^+(Im)(Cl^-) + e^- \rightarrow \mathbf{2}(Im) + Cl^-$	−78.1	−30.2	−108.3	−301.5	−409.8	−0.09	−178.7	−287.0	−1.36
$\mathbf{2}^+(Im)(OAc^-) + e^- \rightarrow \mathbf{2}(OAc^-) + Im$	−185.3	−31.9	−217.2	−199.5	−416.7	−0.01	−120.6	−337.8	−0.83
$\mathbf{2}^+(Im)(MePhO^-) + e^- \rightarrow \mathbf{2}(MePhO^-) + Im$	−235.3	−65.8	−301.0	−187.3	−488.4	0.73	−95.5	−396.5	−0.22
$\mathbf{2}^+(Im)(CH_3S^-) + e^- \rightarrow \mathbf{2}(CH_3S^-) + Im$	−173.0	−57.0	−230.0	−192.7	−422.7	0.05	−99.2	−329.2	−0.92

[a] $E^{\circ\prime}$ ($E^{\circ} = E^{\circ\prime} + 0.41$). [b] HCl instead of $H^+ + Cl^-$. [c] HOAc instead of $H^+ + OAc^-$. [d] ImH^+ instead of $H^+ + Im$.

$$E = E^{\circ} - (RT/F)\ln Q \quad (6)$$

where Q is the reaction quotient specifying concentrations of oxidized and reduced components and other species associated with the chemical change. In the special case that n protons are consumed in solution buffered at pH 7 under otherwise standard conditions, the reaction quotient reduces to $Q = 10^{7n}$ and $E^{\circ\prime} = E^{\circ} - (RT/F)\ln Q = E^{\circ} - 0.41n$ V).[42]

RESULTS

The optimized geometries and calculated data for all systems are collected in Tables S1 and S2 of the Supporting Information. Table 1 collects pertinent geometrical information and spin states for all Fe(II) species. The reactions of **2** with various ligands, based on the MP2 energies, are collected in Table 2. Table 3 examines the reduction potentials for various "Fe(III)"/"Fe(II)" redox couples. Data for the oxidized species are taken from ref 18 except for three hexacoordinated ferric systems which were not part of the earlier study, namely, $\mathbf{2}^+(Im)(OAc^-)$, $\mathbf{2}^+(Im)(Cl^-)$, and $\mathbf{2}^+(Im)((CH_3)_2S)$. The Results and subsequent Discussion refer to MP2-derived data.

Fe(II) PORPHINE COMPLEXES

Structures and Spin States. At the present level of theory, **2** optimizes to D_{4h} symmetry and has ^3E_g ground state in agreement with previous theoretical findings,[10,12] and with the resonance Raman assignment for Fe(II) octaethylporphine.[43] Most other theoretical studies find a $^3A_{2g}$[14−16,44−46] or a $^5A_{1g}$[10] ground state. The experimental findings on Fe(II) tetraphenylporphyrin indicate a $^3A_{2g}$ ground state.[47−49] The two lowest frequency vibrational modes of **2**, 47 and 53 cm^{-1}, correspond to out-of-plane distortions of the porphine ring, while the third, 100 cm^{-1}, is due to the displacement of the iron atom out of the porphine plane. At the B3LYP/6-31+G(d) level, the singlet and quintet states of **2** were higher than the triplet state by 138 and 22 kJ mol^{-1}, respectively.

The gaseous-phase optimized structures of **2**, all pentacoordinate, and a number of hexacoordinate complexes with **2**, are shown in Figures 1 and 2. While **2** is planar, all

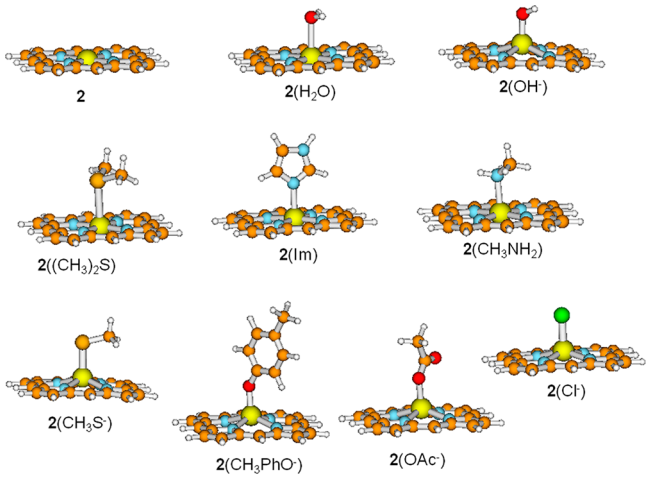

Figure 1. Structures of **2** and its pentacoordinated complexes involved in the present study.

pentacoordinated complexes have the iron out of the porphine plane. The smallest out-of-plane displacement is in the case of $\mathbf{2}(H_2O)$ 0.07 Å, while the largest are for $\mathbf{2}(CH_3S^-)$ 0.64 Å and $\mathbf{2}(OH^-)$ 0.67 Å. The pentacoordinated complexes with neutral ligands and the smaller out-of-plane displacement of the iron atom have intermediate spin, i.e., triplet, ground states. The

dx.doi.org/10.1021/jp305864y | J. Phys. Chem. B 2012, 116, 10301−10310

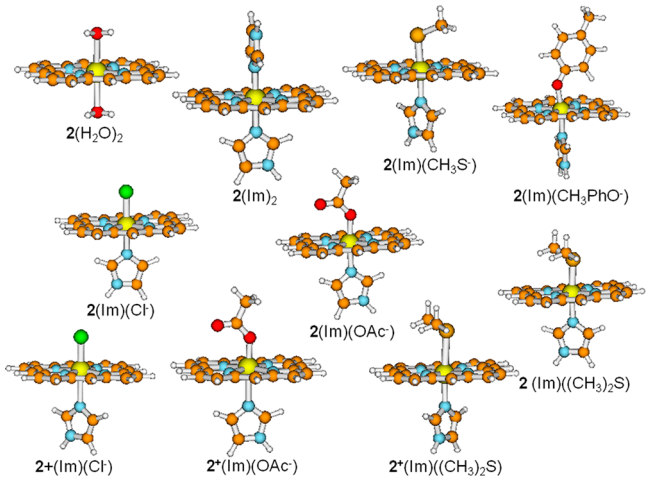

Figure 2. Hexacoordinated complexes of **2** and $\mathbf{2}^+$ involved in the present study.

quintet state of each is within 15 kJ mol^{-1} except in the case of **2**((CH$_3$)$_2$S), 31 kJ mol^{-1}. Singlet states are higher still. The charged ligands induce a greater out-of-plane displacement, and the ground state is quintet rather than triplet which is 25−40 kJ mol^{-1} higher. Singlet states are 20−40 kJ mol^{-1} higher still.

We examined only a number of hexacoordinate complexes of the type **2**(L)(L′), where L and L′ are selected combinations of the six ligands = H$_2$O, CH$_3$S$^-$, Cl$^-$, Im, (CH$_3$)$_2$S, OAc$^-$, or CH$_3$PhO$^-$. These are listed in Table 1 and shown in Figure 2. The ground state of **2**(H$_2$O) is triplet, with the singlet state being about 20 kJ mol^{-1} higher. The ground states of **2**(Im)$_2$ and **2**(Im)((CH$_3$)$_2$S) are singlet, with the triplet and quintet states being similar in energy and about 35 and 12 kJ mol^{-1}, respectively, higher. The ground state of **2**(Im)(Cl$^-$) is also singlet, lying 74 kJ mol^{-1} below the quintet and 275 kJ mol^{-1} below the triplet. On the basis of the result for the chloro derivative, we assumed that the ground states of **2**(Im)(CH$_3$S$^-$), **2**(Im)(OAc$^-$), and **2**(Im)(CH$_3$PhO$^-$) are also singlets. The hexacoordinated structures listed in Table 1 are local minima in the gaseous phase. As discussed below, many are not stable in aqueous or benzene solution. Attempts to locate hexacoordinated structures of **2**(Im) and **2**(CH$_3$S$^-$) with H$_2$O in the gaseous phase yielded structures in which the water was H-bonded to one of the ring N atoms and not coordinated to the iron. Although we did not verify it, we expect the same to be true of **2**(OAc$^-$) and **2**(CH$_3$PhO$^-$).

Stability of the Complexes of 2 in Hydrophobic Media (Benzene). The IEFPCM procedure was applied to the gaseous-phase-optimized geometries to estimate stability in benzene (dielectric constant ε = 2.27). The free energies of solvation by benzene, and consequent free energies of reaction in benzene, are listed as the last two columns of Table 2.

As mentioned in the Introduction, experimental data for equilibria of the type shown in eqs 1 and 2 are available for a number of hemochromes, which display the unusual feature that the second binding constant, K_2, is greater than the first, K_1. Deuteroheme, **3**, is the closest analogue of **2** for which we could find data. The equilibrium data for **3** imply ΔG_1 = −20.8 kJ mol^{-1}, ΔG_2 = −27.6 kJ mol^{-1} in benzene at 298 K (eqs 1 and 2). If **2** is a suitable model for **1** and **3**, then the calculated values for **2**(Im) and **2**(Im)$_2$ in the gaseous phase and in a continuum model of benzene (ε = 2.27) should reproduce these features. The results with **2**(Im) and **2**(Im)$_2$ confirm that the ground states are triplet and singlet, respectively (Table 1), and indicate that the enthalpy change for the second addition of Im, ΔH_2(**2**(Im)$_2$) = −126 kJ mol^{-1}, is more negative than the first, ΔH_1(**2**(Im)$_2$) = −89 kJ mol^{-1} (Table 2). The combination of unfavorable entropy and solvation yields $\Delta G_{(bz)}$(**2**(Im)) = −29 kJ mol^{-1} and $\Delta G_{(bz)}$(**2**(Im)$_2$) = −43 kJ mol^{-1} (Table 2), in qualitative agreement with experimental values for **3**. We note that the calculated values for **2** are underestimated by a large amount at the B3LYP/LB//B3LYP/SB level of theory, by 77 and 88 kJ mol^{-1}, respectively.[18]

In summary, the data shown in Table 2 are derived from "MP2/LB"//B3LYP/SB enthalpies, with all thermal and solvation corrections derived at the B3LYP/SB level. Table 2 should be viewed as giving binding affinities that are more accurate in the relative sense than in the absolute sense. Of the negatively charged species, the most strongly bound is OH$^-$ ($\Delta H_{(g)}$(298K) = −299 kJ mol^{-1}), followed by CH$_3$S$^-$ (−286 kJ mol^{-1}), CH$_3$PhO$^-$ (−270 kJ mol^{-1}), Cl$^-$ (−247 kJ mol^{-1}), and CH$_3$CO$_2^-$ (−216 kJ mol^{-1}). Of the neutral species, the strongest bound is imidazole, a model for histidine ($\Delta H_{(g)}$(298K) = −89 kJ mol^{-1}), followed by CH$_3$NH$_2$, a model for lysine, and (CH$_3$)$_2$S, a model for methionine (both −72 kJ mol^{-1}). Water is the least strongly bound (−37 kJ mol^{-1}). We know from the above considerations that the binding of imidazole, and possibly the others as well, is overestimated by about 12 kJ mol^{-1}.

From the relative free energies of binding in benzene (last column of Table 2), one can predict the outcome of displacement reactions, eq 7. In this case, the large error in absolute binding energy applies to both sides of eq 7 and should cancel to some extent.

$$\mathbf{2}(L_1) + L_2 \rightarrow \mathbf{2}(L_2) + L_1 \qquad \Delta G_{bz,(7)} \tag{7}$$

All of the neutral ligands, CH$_3$NH$_2$, Im, and (CH$_3$)$_2$S, will displace water in benzene (eq 7, L$_1$ = H$_2$O).

The lower half of Table 2 lists several addition reactions that yield hexacoordinated species. The enthalpy, and therefore free energy, changes may be subject to a large overestimation, as they were in the case of the hemochrome, **2**(Im)$_2$, discussed above. Addition of a second water to **2**(H$_2$O) to form **2**(H$_2$O)$_2$ is predicted to be endergonic by 15 kJ mol^{-1} due to an unfavorable change in the free energy of solvation. The last three rows are of greater interest in the biological connection where benzene is intended to represent a nonpolar environment. With an imidazole (i.e., a His) in place, addition of a thiolate (CH$_3$S$^-$, i.e., Cys$^-$) is weakly exergonic. However, the reverse is not true. With a Cys as the fifth ligand, addition of an Im is strongly endothermic. Thus, coordination of a thiolate is probably followed by loss of the His coordination. The same is true of addition of a phenolate (i.e., Tyr) and acetate (Glu, Asp, or C-terminus).

Stability of Complexes of 2 in Water. Experimental data for the addition of ligands to Fe(II)/porphyrins in aqueous media seems to be limited to mixed solvents, presumably for solubility reasons. For instance, the combined stability constant, β_2 (=K_1K_2) for eq 8 in aqueous media, is log(β_2) = 4.0, with $K_2 > K_1$.[50]

$$\mathbf{3} + 2\mathrm{Im} \rightarrow \mathbf{3}(\mathrm{Im})_2 \qquad \Delta G_{(aq)(8)} \tag{8}$$

The value log(β_2) = 4.0 implies $\Delta G_{(aq)(8)}$ = −23 kJ mol^{-1}. The calculated analogous value for **2** may be derived from Table 2, $\Delta G_{(aq)(8)}$ = −41 kJ mol^{-1}, in qualitative agreement with

dx.doi.org/10.1021/jp305864y | J. Phys. Chem. B 2012, 116, 10301−10310

experiment. Addition of a single water in the aqueous phase, yielding $\mathbf{2}(H_2O)$, eq 9, is isoergonic, $\Delta G_{(aq)(9)} \approx 0$ kJ mol^{-1}.

$$\mathbf{2} + H_2O \rightarrow \mathbf{2}(H_2O) \qquad \Delta G_{(aq)(9)} \tag{9}$$

Addition of a second water, yielding hexacoordinate $\mathbf{2}(H_2O)_2$, eq 10, is endergonic in water, $\Delta G_{(aq)(10)} = 10$ kJ mol^{-1}.

$$\mathbf{2}(H_2O) + H_2O \rightarrow \mathbf{2}(H_2O)_2 \qquad \Delta G_{(aq)(10)} \tag{10}$$

Thus, we have the interesting prediction that the hexacoordinated bis(imidazole) complex is more stable in water than either the H_2O or Im pentacoordinated complexes, and that the former is less stable than the latter. The low binding affinity of the intermediate complex, $\mathbf{2}$(Im), may explain the inability to observe the intermediate complex $\mathbf{3}$(Im) in eq 8.[50]

The parent, $\mathbf{2}$, binds OH^- strongly in the gaseous phase (eq 11), $\Delta H_{(g)} = -299$ kJ mol^{-1}, and in aqueous solution, addition of OH^- to $\mathbf{2}$ is exergonic, $\Delta G_{(aq)} = -33$ kJ mol^{-1}. However, at pH 7, they become weakly endergonic. The predicted pK_a of $\mathbf{2}(H_2O)$ is 8 (Table 2).

$$\mathbf{2} + OH^- \rightarrow \mathbf{2}(OH^-) \qquad \Delta G_{(aq)(11)} \tag{11}$$

In water, at physiological pH, carboxylates and halides are not protonated. Addition of OAc^- and Cl^- to $\mathbf{2}$ is exergonic, the former weakly, $\Delta G_{(aq)} = -19$ kJ mol^{-1}, the latter comparatively strongly, $\Delta G_{(aq)} = -76$ kJ mol^{-1}. Addition of thiolate and phenolate to $\mathbf{2}$ is also strongly exergonic, but these species are protonated at pH 7, as are amines. Addition must be accompanied by loss of the proton (eq 12).

$$\mathbf{2} + LH \rightarrow \mathbf{2}(L) + H^+ \qquad \Delta G_{(aq)(12)} \tag{12}$$

From the middle of Table 2, one can see that phenols (L = CH_3PhOH) and thiols (L = CH_3SH) will be spontaneously deprotonated upon attachment to $\mathbf{2}$, but amines (L = $CH_3NH_3^+$) and water (L = H_2O) will not.

Hexacoordinated Complexes of 2. We examined five hexacoordinated complexes of $\mathbf{2}$ in addition to $\mathbf{2}(Im)_2$ and $\mathbf{2}(H_2O)_2$. The seven complexes listed in Table 1 and shown in Figure 2 are local minima in the gaseous phase. From Table 1, one notes that the hexacoordinated complexes that have Im as a ligand have singlet ground states.

Table 2 lists a number of addition complexes according to eq 13, where L and L′ are models for His, Glu, Asp, Tyr, Met, and Cys, the most common ligands of hemes in nature.

$$\mathbf{2}(L) + L' \rightarrow \mathbf{2}(L)(L') \qquad \Delta G_{(aq)(13)} \tag{13}$$

If Im is already attached, the charged ligands bind with high exothermicity in the gaseous phase. In water, the addition is accompanied by a highly endergonic change in the free energy of solvation, about 150 kJ mol^{-1} in each case, that cancels the exergonicity of the gaseous-phase reaction. As a result, none of $\mathbf{2}(Im)(OAc^-)$, $\mathbf{2}(Im)(CH_3S^-)$, or $\mathbf{2}(Im)(CH_3PhO^-)$ are predicted to be stable in water. All will lose the Im moiety (i.e., release His). The only hexacoordinated complexes of $\mathbf{2}$ that are stable in water are $\mathbf{2}(Im)_2$ and $\mathbf{2}(Im)((CH_3)_2S)$.

REDUCTION POTENTIALS, $E°$("Fe(III)"/"Fe(II)")

Table 3 presents a series of Fe(III)/Fe(II) redox couples and the predicted standard reduction potentials, $E°$, for the displayed half reactions relative to the standard hydrogen electrode (SHE) in an aqueous environment and in benzene. The present procedures yield very good agreement for the aqueous Fe^{3+}/Fe^{2+} couple, calculated 0.70 V and experimental 0.77 V.[32] Data for the Fe(III) porphine complexes, $\mathbf{2}^+(L_1)(L_2)$, were taken from ref 18.

The predicted reduction potential of the parent system $\mathbf{2}$ serves as a reference against which to judge the effect of additional ligands on the iron: $E°(\mathbf{2}^+/\mathbf{2}) = 0.47$ V in water; $E°(\mathbf{2}^+/\mathbf{2}) = 1.06$ V in benzene. A significant determining factor for the magnitude of $E°$ is the large change of free energy of solvation as the charge of the Fe species is changed by one unit: ≈130 kJ mol^{-1} in water and ≈70 kJ mol^{-1} in benzene for +1 → 0; ≈ −160 kJ mol^{-1} in water and ≈ −80 kJ mol^{-1} in benzene for 0 → −1. In benzene, the changes are smaller than in water, resulting in more positive reduction potentials for a +1 → 0 change and more negative values for a 0 → −1 change. A scan of the aqueous $E°$ values listed in Table 3 (fourth column from last) reveals that, with one exception, all of the reduction potentials of the penta- and hexacoordinated complexes are negative or close to zero versus SHE. The exception, $E°(\mathbf{2}^+(Im)(CH_3PhO^-)/\mathbf{2}(CH_3PhO^-), Im) = 0.73$ V, is discussed below. From the previous study of the penta- and hexacoordinated complexes of $\mathbf{2}^+$,[18] it was found that the charged ligands OH^-, OAc^-, CH_3S^-, and CH_3PhO^- could accommodate the addition of a sixth neutral ligand in water but not a charged one. In some cases, hexacoordinated complexes would only be stable if the entropic penalty (the $-T\Delta S$ term) for their formation was reduced by chelation. In Table 3, we consider reduction of both the most stable penta- and hexacoordinated complexes of $\mathbf{2}^+$ to the analogous complexes of $\mathbf{2}$, as well as cases where the reduction of hexacoordinated complexes of $\mathbf{2}^+$ is accompanied by dissociation of the less tightly bound ligand. In the latter case, the reverse process of oxidation will have a significantly different value than the reduction.

Redox Chemistry of Hemin, $\mathbf{1}^+(Cl^-)$, and Ferrihemic Acid, $\mathbf{1}^+(OH^-)$. The most stable pentacoordinated complex of $\mathbf{2}^+$ is $\mathbf{2}^+(OH^-)$.[18] Its reduction to $\mathbf{2}(OH^-)$ has the most negative reduction potential of the systems studied, $E°(\mathbf{2}^+(OH^-)/\mathbf{2}(OH^-)) = -1.37$ V at pH > 8. The value at pH 7 is similar, $E°'(\mathbf{2}^+(OH^-),H^+/\mathbf{2}(H_2O)) = -1.30$ V. In benzene, the value is much lower, $E°(\mathbf{2}^+(OH^-)/\mathbf{2}(OH^-)) = -2.31$ V. The heme analogue is $\mathbf{1}^+(OH^-)$, known variously as hemic acid, ferrihemic acid, or hematin. Hemin, the chloro complex of heme, $\mathbf{1}^+(Cl^-)$, is modeled by $\mathbf{2}^+(Cl^-)$. Its calculated reduction potential is $E°(\mathbf{2}^+(Cl^-)/\mathbf{2}(Cl^-)) = -0.09$ V. In benzene, the value is lower, $E°(\mathbf{2}^+(Cl^-)/\mathbf{2}(Cl^-)) = -0.95$ V. The electrochemistry of ferrihemic acid and hemin has been investigated several times.[51−54] In 1930, Conant and Tongberg titrated hemin and ferrihemic acid with $TiCl_3$ in aqueous solution and found that $E° = -0.230$ V for both species within the limits of experimental error.[51] This value is clearly inconsistent with the present results that the reduction potentials of the two species differ by more than a volt and bracket the experimental value. The present and previous studies suggest that the reduced form, $\mathbf{2}(Cl^-)$, is more stable than $\mathbf{2}(OH^-)$, while, in the oxidized form, the hydroxide is more stable than the chloride. If hemin hydrolyzes to ferrihemic acid in water and the reduced heme can obtain a chloride ion from the titanous chloride titrating agent, the appropriate reduction process is given by eq 14:

$$\mathbf{2}^+(OH^-) + Cl^- + H^+ + e^- \rightarrow \mathbf{2}(Cl^-) + H_2O \tag{14}$$

for which $E°(\mathbf{2}^+(OH^-), H^+, Cl^-/\mathbf{2}(Cl^-), H_2O) = -0.10$ V, and at pH 7, $E°' = -0.51$ V. Thus, given that $\mathbf{2}$ is a model for $\mathbf{1}$, the

agreement is fair and lends credence to the mechanism of eq 14. Apparently, hemin, $\mathbf{1}^+(Cl^-)$, does not hydrolyze in aqueous liposomes. The measured value, $E = -0.12$ V,[54] is in good agreement with the calculated value, $E^\circ(\mathbf{2}^+(Cl^-)/\mathbf{2}(Cl^-)) = -0.09$ V (Table 3).

The redox properties of hemin together with nitrogen ligands have been measured in methanol solution, in *N*-methylimidazole (NMI) solution, and in methanol with added NMI.[53] In the pure solvent, NMI, the hemin exchanges the Cl^- ion for the NMI forming the hemochrome which in the present study is modeled by $\mathbf{2}^+(Im)_2$. The experimental value, 0.049 V, is intermediate to the calculated value in benzene, $E^\circ(\mathbf{2}^+(Im)_2/\mathbf{2}(Im)_2) = 0.12$ V, and in water, $E^\circ(\mathbf{2}^+(Im)_2/\mathbf{2}(Im)_2) = -0.34$ V, as expected from the intermediate polarity of the solvent NMI.

The reduction potentials for several hemochromes of "heme a" have been measured at pH 7.[55] The bis(imidazole) "heme a" hemochrome had a measured reduction potential of $E^\circ = 0.045$ V. In the present study, the closest analogous reaction is

$$\mathbf{2}^+(Im)_2 + e^- \rightarrow \mathbf{2}(Im)_2 \qquad (15)$$

for which $E^\circ(\mathbf{2}^+(Im)_2/\mathbf{2}(Im)_2) = -0.34$ V. The low value arises from the large loss of free energy of solvation. $\Delta\Delta G_{solv} = 112$ kJ mol^{-1}. It is likely that the combination of the large hydrophobic farnesyl group and two carboxylate groups of "heme a" would reduce the value of $\Delta\Delta G_{solv}$ to a lower value, more akin to the situation in benzene solvent. In benzene, $\Delta\Delta\Delta G_{solv} = 67$ kJ mol^{-1} and $E^\circ(\mathbf{2}^+(Im)_2/\mathbf{2}(Im)_2) = 0.12$ V (Table 3). Hemin titrated with imidazole and 1-methylimidazole to form the hemochromes in aqueous liposomes had reduction potentials of −0.17 and −0.16 V, respectively.[54] Again, these values are intermediate to the values in water and benzene, and reflect the hydrophobic nature of aqueous liposomes.

DISCUSSION

It is clear from the data in Table 3 of the previous paper[18] that, in aqueous media, hydroxide is the best ligand for Fe(III) porphine $\mathbf{2}^+$, and that the appropriate description of the Fe(III) porphine is as the pentacoordinated hydroxy complex, $\mathbf{2}^+(OH^-)$, the model for hemic acid, at pH 7. The computations indicate that, of the other ligands considered here, only thiolate and acetate will displace the single bound hydroxide from $\mathbf{2}^+(OH^-)$ to form the corresponding pentacoordinated complex. The present results (Table 2) indicate that Fe(II) porphine **2** is only weakly complexed to water and, with the exception of amines, any of the other ligands can form pentacoordinated complexes. Two pairs, Im + Im and Im + $(CH_3)_2S$, can also form stable hexacoordinated complexes with **2** in water. By implication, these should be the most common forms of attachment of noncovalently bound heme in biological systems. B-type cytochromes contain a noncovalently bound heme prosthetic group exposed to the aqueous cytoplasm, linked by two His residues or His and Met.[56] The prediction from the calculations is that the reduction potential of Fe(III) porphine will have a value that is dependent on other ligands, X, that may be present in solution:

$$\mathbf{2}^+(OH^-) + X^- + H^+ + e^- \rightarrow \mathbf{2}(X^-) + H_2O \qquad (16a)$$

$$\mathbf{2}^+(OH^-) + XH + e^- \rightarrow \mathbf{2}(X^-) + H_2O \qquad (16b)$$

Thus, $E^\circ(\mathbf{2}^+(OH^-), X, H^+/\mathbf{2}(X) + H_2O)$: X = Cl^-, $E^{\circ\prime} = -0.51$ V; OAc^-, $E^{\circ\prime} = -1.11$ V; X = Im, $E^{\circ\prime} = -1.15$ V; X = CH_3SH, $E^\circ = -0.46$ V; X = CH_3PhOH, $E^\circ = -0.61$ V. Unfortunately, we have not been able to find any experimental redox data on the parent iron porphine systems. Earlier computational studies have addressed the spin states and geometries of **2** and $\mathbf{2}^+$ and various complexes,[10−12,14,19,44,57,58] but none have examined the binding of the bioavailable ligands to either **2** or $\mathbf{2}^+$. Since data for the parent compounds do not seem to exist, one then must ask, why not, and what is the relevance of the present study to the properties of more highly substituted iron porphyrin complexes?

Lessons from Biological Systems. In aerobic biological systems, iron is redox cycled between the more stable Fe(III) form and the more active Fe(II) form.[59] The multicopper protein, ceruloplasmin, has been identified as a ferroxidase,[60] while the role of ferryl reductase is played by metalloreductases like Dcytb, which, like all metalloreductases, is a b-type cytochrome and likely NADPH-dependent. Cytochrome b-562 with His and Met ligating groups has $E_m = +110$ mV. The same ligands are in class I c-type cytochromes which have $E_m \approx +230$ to +270 mV. Cytochrome c(2) has a higher redox potential still, +350 mV.[61] Equation 17 models the reduction of cytochromes that have a hexacoordinated heme with coordinated His and Met residues:

$$\mathbf{2}^+(Im)((CH_3)_2S) + e^- \rightarrow \mathbf{2}(Im)((CH_3)_2S) \qquad (17)$$

$E^\circ(\mathbf{2}^+(Im)((CH_3)_2S)/\mathbf{2}(Im)((CH_3)_2S)) = -0.51$ V in water, and $E^\circ(\mathbf{2}^+(Im)((CH_3)_2S)/\mathbf{2}(Im)((CH_3)_2S)) = 0.22$ V in benzene. The reduction potential calculated in a fully hydrated environment is incompatible with the midpoint potentials of either b-type or c-type cytochromes with methionine ligands. However, the value calculated in benzene is close to the experimental value for c-type cytochromes, suggesting that the heme is in a hydrophobic pocket. It also suggests that the hemes in b-type cytochromes are more solvent exposed than c-type, since their reduction potentials are lower.

Cytochrome c is a small (about 100 residues), ubiquitous, heme-containing protein involved in the respiratory chain in mitochondria. Its heme prosthetic group is covalently attached via thioether linkages formed by addition of two cysteinyl thiol groups to the vinyl groups of the heme. In such a small protein, the heme group would be largely exposed to the solvent and would be readily lost were it not for the covalent attachment. The same is true for *N*-acetylmicroperoxidase-8 (NAcMP8), $\mathbf{4}^+$,[62] the octapeptide fragment of cytochrome c which contains the heme. The heme of $\mathbf{4}^+$ has a fifth ligand, the imidazole of a histidine ($\mathbf{4}^+(Im)$), and is considered to have an exchangeable sixth ligand, water. The reduction potentials of cytochrome c and $\mathbf{4}^+(Im)$ are relatively insensitive to ligands which can be exchanged for the water. Both the ferrous form, $\mathbf{4}(Im)$, and the ferric form, $\mathbf{4}^+(Im)$, coordinate imidazole as a sixth ligand, the latter more strongly than the former, $\log K = 4.08$ vs $\log K = 3.40$.[63] The reduction potentials of $\mathbf{4}^+(Im)_2$ have been reported, −0.20 V. The analogous compound here is $\mathbf{2}^+(Im)_2$, which was discussed above, $E^\circ(\mathbf{2}^+(Im)_2/\mathbf{2}(Im)_2) = -0.34$ V. The value is lower than observed for $\mathbf{4}^+(Im)_2$, but the low value confirms that the heme is exposed to the aqueous environment, since the value in benzene for $\mathbf{2}^+(Im)_2$ is considerably higher, 0.12 V (Table 3). Anionic ligands also coordinate to $\mathbf{4}^+(Im)$, one of which is modeled by $\mathbf{2}^+(Im)(Cl^-)$. The predicted reduction potential for $\mathbf{2}^+(Im)(Cl^-)$ in water assuming the Cl^- remains attached to the heme, $E^\circ(\mathbf{2}^+(Im)(Cl^-)/\mathbf{2}(Im)(Cl^-)) = -0.77$ V, is considerably lower than observed for $\mathbf{4}^+(Im)(Cl^-)$, −0.15 V. The data in Table 2 indicate that both $\mathbf{2}^+(Im)(Cl^-)$ and

$\mathbf{2}(\mathrm{Im})(\mathrm{Cl}^-)$ are unstable toward dissociation in water. However, experimentally, $\mathbf{4}^+(\mathrm{Im})$ was found to have a low affinity for Cl^-, K = 0.69. Nevertheless, it is likely that the reduced form would release the Cl^-, as modeled by eq 18:

$$\mathbf{2}^+(\mathrm{Im})(\mathrm{Cl}^-) + \mathrm{e}^- \rightarrow \mathbf{2}(\mathrm{Im}) + \mathrm{Cl}^- \quad (18)$$

Indeed, $E^\circ(\mathbf{2}^+(\mathrm{Im})(\mathrm{Cl}^-)/\mathbf{2}(\mathrm{Im}) + \mathrm{Cl}^-) = -0.06$ V is in reasonable agreement with the observed value for $\mathbf{4}^+(\mathrm{Im})(\mathrm{Cl}^-)$, −0.15 V.

Horse radish peroxidase contains a heme prosthetic group attached to a single His residue. The sixth coordination site is vacant and serves as the active site. The resting form is the ferri form, and ferri/ferro redox cycling is not involved in its native peroxidase activity. The reduction potential of the heme prosthetic group is −0.30 V.[64] The redox process is simply modeled by

$$\mathbf{2}^+(\mathrm{Im}) + \mathrm{e}^- \rightarrow \mathbf{2}(\mathrm{Im}) \quad (19)$$

for which $E^\circ(\mathbf{2}^+(\mathrm{Im})/\mathbf{2}(\mathrm{Im})) = -0.34$ V in water and +0.10 V in benzene. The value is very close to that predicted in water, which is surprising, since the crystal structure of horse radish peroxidase shows the heme residing in the middle of a cluster of alpha helices and beta sheets and "solvated" by only two water molecules.[65,66]

Catalase peroxidases and cytochrome c peroxidase also contain a heme prosthetic group attached to a single His residue. The distal face of the heme has nonbonded tryptophan and histidine residues partially shielding that face. Reduction potentials, modeled by eq 19, are negative, although less so than horse radish peroxidase. For instance, MagKatG1 and MagKatG2 from the fungus *Magnaporthe grisea* have standard reduction potentials, −0.186[67] and −0.220 V,[68] respectively. The value of the reduction potential of yeast cytochrome c peroxidase, −0.180 V, has been shown to be dependent on electrostatic interactions with neighboring groups in the environment.[69]

Cytochrome P450 is a ubiquitous superfamily of heme-containing proteins in which the heme is coordinated via a thiolate ligand. The resting form is formally a high spin ferric form, modeled in the present study as $\mathbf{2}^+(\mathrm{CH_3S}^-)$. It has been suggested that there is a linear free energy relationship between the spin state induced by bound substrates and the redox potential,[70] but this is not the case with most membrane bound cytochrome P450s.[71] In the previous study of adducts of $\mathbf{2}^+$, it was found that none of the limited set of ligands would add to $\mathbf{2}^+(\mathrm{CH_3S}^-)$ to form a stable hexacoordinated adduct in water or benzene.[18] For example, addition of Im to $\mathbf{2}^+(\mathrm{CH_3S}^-)$ yields $\mathbf{2}^+(\mathrm{CH_3S}^-)(\mathrm{Im})$ in a doublet ground state in the gaseous phase, but the addition is endergonic in water, $\Delta G_{(\mathrm{aq})}$ = 64 kJ mol^{-1}, and in benzene, $\Delta G_{(\mathrm{bz})}$ = 53 kJ mol^{-1}.[18] In the absence of a sixth ligand, reduction of the most stable $\mathbf{2}^+(\mathrm{CH_3S}^-)$ — hextet — to the most stable $\mathbf{2}(\mathrm{CH_3S}^-)$ — quintet — is predicted to be very negative, $E^\circ(\mathbf{2}^+(\mathrm{CH_3S}^-)/\mathbf{2}(\mathrm{CH_3S}^-)) = -0.61$ V, in water and even more so, −1.47 V, in benzene. The lower value in the hydrophobic solvent ensues from the higher solvent stabilization of the charged reduced species in water, $\Delta\Delta G_{\mathrm{solv}}(\mathrm{aq}) = -165.7$ kJ mol^{-1} vs $\Delta\Delta G_{\mathrm{solv}}(\mathrm{bz}) = -82.7$ kJ mol^{-1} (Table 3). The thiolate ligand is a strong reducing agent, so in effect, the ferric iron in $\mathbf{2}^+(\mathrm{CH_3S}^-)$ is already in reduced form. Although the spin state is formally hextet, the spin density on the iron atom is 4.00, i.e., quintet. Reduction to $\mathbf{2}(\mathrm{CH_3S}^-)$ leaves the iron atom essentially unchanged with spin density 3.67 and the positive charge reduced by only 0.15*e*. Most of the added electron is divided between the thiolate ligand, 0.27*e*, and the porphine ring, 0.58*e*, as has been previously observed computationally.[72]

By contrast, the cytochrome P450 oxidative cycle begins with the binding of a substrate into the enzyme active site which is close to the heme prosthetic group. Apparently, addition of the substrate lowers the spin multiplicity and raises the reduction potential into the −0.2 to −0.3 V range,[70c] so that the complex can be reduced by an NADPH cofactor. The cycle proceeds with the reduced heme attaching O_2. The measured value of cytochrome P450 3A4, bound to carbon nanodiscs, is −0.22 V,[73] substantially higher than that of (ligand-free) $\mathbf{2}^+(\mathrm{CH_3S}^-)$. If the Im in $\mathbf{2}^+(\mathrm{CH_3S}^-)(\mathrm{Im})$ is considered to be held in place by the enzyme in both the oxidized and reduced forms, the predicted reduction potential is even more negative, $E^\circ(\mathbf{2}^+(\mathrm{CH_3S}^-)(\mathrm{Im})/\mathbf{2}(\mathrm{CH_3S}^-)(\mathrm{Im})) = -1.37$ V, in water and even more so, −2.27 V, in benzene. The reason is that $\mathbf{2}(\mathrm{CH_3S}^-)(\mathrm{Im})$ is even less stable toward dissociation than is the oxidized form (Table 2). The most likely scenario for the ligand promoted reduction of cytochrome P450 is that the ligand is held in place by the enzyme in the *oxidized* form but is released in whole or in part in the reduced form, viz., eq 20:

$$\mathbf{2}^+(\mathrm{CH_3S}^-)(\mathrm{Im}) + \mathrm{e}^- \rightarrow \mathbf{2}(\mathrm{CH_3S}^-) + \mathrm{Im} \quad (20)$$

For eq 20, $E^\circ(\mathbf{2}^+(\mathrm{CH_3S}^-)(\mathrm{Im})/\mathbf{2}(\mathrm{CH_3S}^-) + \mathrm{Im}) = 0.05$ V in water and −0.92 V in benzene (Table 3). If the ligand is only partially removed from the heme in the reduced form, the reduction potential would be lower and in closer agreement with the experimental range. The persistent low value in benzene implies that the heme is not in a fully hydrophobic environment but is exposed to the aqueous environment to some extent. The crystal structure of human cytochrome P450 2D6 bears this out.[74] There is no water molecule in the sixth coordination site, but the large active site cavity situated above the heme has two carboxylate groups and is solvent (and substrate) accessible.

Catalase is a ubiquitous hemoprotein that dismutates H_2O_2 into H_2O and O_2. Its heme has a Tyr ligand as the fifth ligand for the iron. The properties of phenolate as a ligand are very similar to those of thiolate discussed above. The resting form is formally a high spin ferric form, modeled in the present study as $\mathbf{2}^+(\mathrm{CH_3PhO}^-)$. It was previously found that none of the ligands would add to $\mathbf{2}^+(\mathrm{CH_3PhO}^-)$ to form a stable hexacoordinated adduct in water or benzene.[18] For instance, the addition of Im (i.e., His) to $\mathbf{2}^+(\mathrm{CH_3PhO}^-)$ is highly endergonic in water, $\Delta G_{(\mathrm{aq})}$ = 130 kJ mol^{-1}, and in benzene, $\Delta G_{(\mathrm{bz})}$ = 120 kJ mol^{-1}.

$$\mathbf{2}^+(\mathrm{CH_3PhO}^-) + \mathrm{e}^- \rightarrow \mathbf{2}(\mathrm{CH_3PhO}^-) \quad (21)$$

Direct reduction according to eq 21 has values almost identical to the thiolate case, $E^\circ(\mathbf{2}^+(\mathrm{CH_3PhO}^-)/\mathbf{2}(\mathrm{CH_3PhO}^-)) = -0.62$ V in water and −1.47 V in benzene. Like thiolate, phenolate attached to Fe(III) effectively reduces it to Fe(II), with similar spin densities, 4.10 and 3.67, respectively. The higher endothermicity for attachment of a sixth ligand to the Tyr-bound porphyrin compared to the Cys-bound one makes it unlikely that the enzyme framework could hold one sufficiently close to raise the reduction potential, so that a scenario analogous to eq 20 is unlikely. Not surprisingly then, unlike in the case of cytochrome P450, reduction of the formal Fe(III) species is not necessary for the catalytic activity of catalases.

dx.doi.org/10.1021/jp305864y | J. Phys. Chem. B 2012, 116, 10301−10310

Rather, the Fe(III) species acts as a *reducing* agent toward H_2O_2 and is further oxidized to a formal Fe(IV) oxo species.[75]

CONCLUSIONS

Models of the side chains of the naturally occurring amino acids were examined for their affinity for ferroporphine, **2**. With two exceptions, **2**(Im)$_2$ and **2**(Im)((CH$_3$)$_2$S), the complexes are predicted to be pentacoordinated in water (Table 2). The most stable are with the anionic ligands, **2**(Cl$^-$), **2**(CH$_3$PhO$^-$), and **2**(CH$_3$S$^-$). The parent **2** has significantly lower affinity for both OH$^-$ and AcO$^-$, largely due to loss of free energy of solvation of the small anionic species as a result of complexation. The neutral ligands, CH$_3$NH$_2$, Im, (CH$_3$)$_2$S, and even water, have lower than millimolar affinity. The two stable hexacoordinated species are predicted to have greater than millimolar affinity. In the biological context, ferroheme **1** cannot be bound solely by virtue of ligation to His (Im), Lys (CH$_3$NH$_2$), or Met ((CH$_3$)$_2$S). Since His *is* a common ligand for heme in enzymes, additional binding is required, either through addition coordination to His or Met, covalent addition to the vinyl groups, salt bridges to the propylcarboxy groups, or hydrophobic interactions. Binding solely to Cys (CH$_3$S$^-$) (e.g., the cytochromes) or Tyr (CH$_3$PhO$^-$) (e.g., catalases) *is* sufficient to yield stable complexes with binding in the pico- or femtomolar range even when exposed to the aqueous environment.

The data from ref 18 was combined with the present data to examine the redox chemistry of the iron porphine species in both aqueous and nonpolar (benzene) environments (Table 3). The difference between the two environments is dominated by the differences in the free energy of solvation of the ionic species. Stabilization of ionic species is much higher in water than in benzene with the consequence that reduction of a ferri complex with a neutral ligand, **2**$^+$(L), yields a more positive (or less negative) reduction potential in benzene compared to water. The opposite is true in the case of reduction of a ferri complex with an anionic ligand, **2**$^+$(L$^-$). In this case, stabilization of the anionic reduced product, **2**(L$^-$), is not as great in benzene as it is in water, with the result that the reduction potential is more negative in the nonpolar environment.

The fourth-from-last column of Table 3 lists predicted reduction potentials of a variety of "Fe(III)"/"Fe(II)" complexes in water. The corresponding data in benzene are listed in the last column. With the exception of the parent couple, **2**$^+$/**2**, all of the redox couples examined in water are negative relative to the standard hydrogen electrode (SHE). Pentacoordinated complexes with a neutral ligand and hexacoordinated complexes with two neutral ligands yield positive (vs SHE) reduction potentials in benzene.

The present results are compatible with the current thinking about the activity of some of the common heme-containing enzymes, as discussed above in the case of the peroxidases and the b- and c-type cytochromes, all of which have His ligating groups. Cytochrome P450s and catalase are special cases, since they have highly electron-releasing groups as ligands. Ligation by either thiolate or phenoxide effectively reduces the iron center from Fe(III) to Fe(II) by substantial electron transfer, thus making it not amenable for further reduction. Cytochrome P450s which have a single thiolate ligand from Cys would have too negative a reduction potential to be reduced by the cofactor NADPH were it not for the endergonic imposition of a sixth ligand by the enzyme framework. The free energy gained by (partial) release of this ligand is enough to raise the reduction potential into the active range. This mechanism for raising the reduction potential is not available to catalases, which have a ligating phenoxy group from a Tyr residue, since addition of a sixth ligand is even more endergonic. In fact, the formal Fe(III) center acts as a reducing agent toward hydrogen peroxide and is further oxidized.

ASSOCIATED CONTENT

Supporting Information

The coordinates of all structures discussed together with the energies of the lowest spin states are presented in Table S1. Primary computed data for all the stationary points is listed in Table S2. This material is available free of charge via the Internet at http://pubs.acs.org.

AUTHOR INFORMATION

Corresponding Author

*E-mail: rauk@ucalgary.ca.

Notes

The authors declare no competing financial interest.

ACKNOWLEDGMENTS

We thank the Natural Sciences and Engineering Council of Canada (NSERC) for financial support of this work and Westgrid for generous allocations of computational resources.

REFERENCES

(1) Baer, B. R.; Schuman, J. T.; Campbell, A. P.; Cheeseman, M. J.; Nakano, M.; Moguilevsky, N.; Kunze, K. L.; Rettie, A. E. *Biochemistry* **2005**, *44*, 13914−13920.
(2) Swanson, B. A.; Dutton, D. R.; Lunetta, J. M.; Yang, C. S.; Ortiz de Montellano, P. R. *J. Biol. Chem.* **1991**, *266*, 19258−19264.
(3) Sato, T.; Tanaka, N.; Neva, S.; Funasaki, N.; Iizuka, T.; Shiro, Y. *Biochim. Biophys. Acta* **1992**, *1121*, 1−7.
(4) Marques, H. M.; Cukrowski, I.; Vashi, P. R. *J. Chem. Soc., Dalton Trans.* **2000**, 1335−1342.
(5) Marques, H. M. *Dalton Trans.* **2007**, 4371−4385.
(6) Nicholls, P.; Fita, I.; Loewen, P. C. *Adv. Inorg. Chem.* **2001**, *51*, 51−106.
(7) Atamna, H; Boyle, K. *Proc. Natl. Acad. Sci. U.S.A.* **2006**, *103*, 3381−3386.
(8) Pramanik, D.; Ghosh, C.; Ghosh Dey, S. *J. Am. Chem. Soc.* **2011**, *133*, 15545−15552.
(9) Atamna, H.; Frey, W. H., II; Ko, N. *Arch. Biochem. Biophys.* **2009**, *487*, 59−65.
(10) Choe, Y.-K.; Hashimoto, T.; Nakano, H.; Hirao, K. *Chem. Phys. Lett.* **1998**, *295*, 380−388.
(11) Rydberg, P.; Olsen, L. *J. Phys. Chem. A* **2009**, *113*, 11949−11953.
(12) Groenhof, A. R.; Swart, M.; Ehlers, A. W.; Lammertsma, K. *J. Phys. Chem. A* **2005**, *109*, 3411−3417.
(13) Rydberg, P.; Sigfridsson, E.; Ryde, U. *J. Biol. Inorg. Chem.* **2004**, *9*, 203−223.
(14) Liao, M.-S.; Watts, J. D.; Huang, M.-J. *J. Comput. Chem.* **2006**, *27*, 1577−1592.
(15) Kozlowski, P. M.; Spiro, G.; Berces, A.; Zgierski, M. Z. *J. Phys. Chem. B* **1998**, *102*, 2603−2608.
(16) Liao, M.-S.; Scheiner, S. *J. Chem. Phys.* **2002**, *116*, 3635−3645.
(17) Conradie, J.; Ghosh, A. *Inorg. Chem.* **2006**, *45*, 4902−4909.
(18) Wondimagegn, T.; Rauk, A. *J. Phys. Chem. B* **2011**, *115*, 569−579.
(19) Bikiel, D. E.; Bari, S. E.; Doctorovich, F.; Estrin, D. A. *J. Inorg. Biochem.* **2008**, *102*, 70−76.
(20) *The Porphyrin Handbook*; Kadish, K. M., Smith, K. M., Guilard, R., Eds.; Academic Press: San Diego, CA, 2000; Vol. *7*, pp 1−78.

(21) Tabata, M.; Nishimoto, J. In *The Porphyrin Handbook*; Kadish, K. M., Smith, K. M., Guilard, R., Eds.; Academic Press: San Diego, CA, 2000; Vol. *9*, p 221.
(22) Perry, C. B.; Chick, T.; Ntlokwana, A.; Davies, G.; Marques, H. M. *J. Chem. Soc., Dalton Trans.* **2002**, 449−457.
(23) Brault, D.; Rougee, M. *Biochem. Biophys. Res. Commun.* **1974**, *57*, 654−659.
(24) Brault, D.; Rouge, M. *Biochemistry* **1974**, *13*, 4591−4597.
(25) Yang, Q.-Z.; Khvostichenko, D.; Atkinson, J. D.; Boulatov, R. *J. Chem. Soc., Chem. Commun.* **2008**, 963−965.
(26) Harbury, H. A. *J. Biol. Chem.* **1957**, *225*, 1009−1024.
(27) Ayala, M; Roman, R; Vazquez-Duhalt, R. *Biochem. Biophys. Res. Commun.* **2007**, *357*, 804−808.
(28) Frisch, M. J.; Trucks, G. W.; Schlegel, H. B.; Scuseria, G. E.; Robb, M. A.; Cheeseman, J. R.; Montgomery, J. A., Jr.; Vreven, T.; Kudin, K. N.; Burant, J. C.; et al. *Gaussian 03*, revision E.01; Gaussian, Inc.: Wallingford, CT, 2004.
(29) Frisch, M. J.; Trucks, G. W.; Schlegel, H. B.; Scuseria, G. E.; Robb, M. A.; Cheeseman, J. R.; Scalmani, G.; Barone, V.; Mennucci, B.; Petersson, G. A.; et al. *Gaussian 09*, revision A.02; Gaussian, Inc.: Wallingford, CT, 2009.
(30) Hertwig, R. H.; Koch, W. *Chem. Phys. Lett.* **1997**, *268*, 345−351.
(31) Scott, A. P.; Radom., L. *J. Phys. Chem.* **1996**, *100*, 16502−16513.
(32) Ali-Torres, J.; Rodriguez-Santiago, L.; Sodupe, M.; Rauk, A. *J. Phys. Chem. A* **2011**, *115* (45), 12523−12530.
(33) Azimi, S.; Rauk, A. *Int. J. Azheimer's Dis.* **2011**, Article ID 539762, 15 pages. DOI: 10.4061/2011/539762.
(34) Paizs, B.; Suhai, S. *J. Comput. Chem.* **1997**, *19*, 575−584.
(35) Bryantsev, V. S.; Diallo, M. S.; van Duin, A. C. T.; Goddard, W. A., III. *J. Chem. Theory Comput.* **2009**, *5*, 1016−1026.
(36) Tomasi, J.; Mennucci, M.; Cances, E. *J. Mol. Struct.: THEOCHEM* **1999**, *464*, 211−226.
(37) Cramer, C. J.; Truhlar, D. G. *J. Comput.-Aided Mol. Des.* **1992**, *6*, 629.
(38) Calculated as the difference between $\Delta_f G_{(g)}(H_2O)$ and $\Delta_f G_{(l)}(H_2O)$, corrected to the standard state of 1 M. The IEFPCM calculated value for water is $\Delta_f G_{solv}(H_2O) = -30.3$ kJ/mol.
(39) Liptak, M. D.; Gross, K. C.; Seybold, P. G.; Feldus, S.; Shields, J. C. *J. Am. Chem. Soc.* **2002**, *124*, 6421−6247.
(40) Ryde, U.; Olsson, M. H. M. *Int. J. Quantum Chem.* **2001**, *81*, 335−347.
(41) 418 kJ mol^{-1} is the Gibbs free energy for the half-reaction, $^1/_2H_{2(g)} \rightarrow H_{(aq)}^+ + e^-$. It can be obtained by adding $\Delta_f G^\circ_{(g)}(H^+) = 1517$ kJ mol^{-1}, $\Delta G_{solv}(H^+) = -1107$ kJ mol^{-1}, and the factor to change the $H_{(aq)}^+$ reference state to 1 M, $-RT\ln(1/24.6) = 8$ kJ mol^{-1}. Additionally, $\Delta_f G^\circ_{(g)}(H^+) = 1517$ kJ mol^{-1} is computed from $\Delta_f G^\circ_{(g)}(H) = 203$ kJ mol^{-1} plus $\Delta_f G^\circ_{(g)}(H^+ + e^-) = 1314$ kJ mol^{-1}.
(42) Hewitt, N.; Rauk, A. *J. Phys. Chem. B* **2009**, *113*, 1202−1209.
(43) Kitagawa, T.; Teraoka, J. *Chem. Phys. Lett.* **1979**, *63*, 443−446.
(44) Rovira, C.; Kunc, K.; Hutter, J.; Ballone, P.; Parrinello, M. *J. Phys. Chem. A* **1997**, *101*, 8914−8925.
(45) Ugalde, J. M.; Dunietz, B.; Dreuw, A.; Head-Gordon, M.; Boyd, R. J. *J. Phys. Chem. A* **2004**, *108*, 4653−4657.
(46) Liao, M.-S.; Huang, M.-J.; Watts, J. D. *J. Phys. Chem. A* **2010**, *114*, 9554−9569.
(47) Collman, J. P.; Hoard, J. L.; Kim, N.; Lang, G.; Reed, C. A. *J. Am. Chem. Soc.* **1975**, *97*, 2676−2681.
(48) Goff, H.; La Mar, G. N.; Reed, C. A. *J. Am. Chem. Soc.* **1977**, *99*, 3641−3646.
(49) Lang, G.; Spartalian, K.; Reed, C. A.; Collman, J. P. *J. Chem. Phys.* **1978**, *69*, 5424−5427.
(50) Al-Jaff, G.; Silver, J.; Wilson, M. T. *Inorg. Chim. Acta* **1990**, *176*, 307−316.
(51) Conant, J. B.; Tongberg, C. O. *J. Biol. Chem.* **1930**, *86*, 733−741.
(52) Tsuchida, E.; Honda, K. *Chem. Lett.* **1975**, 119−122.
(53) Compton, D. L.; Laszlo, J. A. *J. Electroanal. Chem.* **2002**, *520*, 71−78.
(54) Das, D. K; Das, B; Medhi, O. K. *J. Surf. Sci. Technol.* **2008**, *24*, 79−86.
(55) Vanderkooi, G.; Stotz, E. *J. Biol. Chem.* **1966**, *241*, 3316−3323.
(56) von Jagow, G.; Sebald, W. *Annu. Rev. Biochem.* **1980**, *49*, 281−314.
(57) Khvostichenko, D.; Choi, A.; Boulatov, R. *J. Phys. Chem. A* **2008**, *112*, 3700−3711.
(58) Abdurahman, A.l; Renger, T. *J. Phys. Chem. A* **2009**, *113*, 9202−9206.
(59) Kosman, D. J. *J. Biol. Chem.* **2010**, *285*, 26729−26735.
(60) Osaki, S.; Johnson, D. A.; Frieden, E. *J. Biol. Chem.* **1966**, *241*, 2746−2751.
(61) Geremia, S; Garau, G; Vaccari, L; Sgarra, R.; Viezzoli, M. S.; Calligaris, M.; Sgarra, R.; Viezzoli, M. S.; Calligaris, M.; Randaccio, L. *Protein Sci.* **2002**, *11*, 6−17.
(62) Munro, O. Q.; Marques, H. M. *Inorg. Chem.* **1996**, *35*, 3752−3767.
(63) Vashi, P. R.; Marques, H. M. *J. Inorg. Biochem.* **2004**, *98*, 1471−1482.
(64) Harbury, H. A. *J. Biol. Chem.* **1957**, *225*, 1009.
(65) Berglund, G. I.; Carlsson, G. H.; Smith, A. T.; Szöke, H.; Henriksen, A.; Hajdu, J. *Nature* **2002**, *417*, 463−468.
(66) Gajhede., M. *Biochem. Soc. Trans.* **2001**, *29*, 91−99.
(67) Zamocky, M.; Furtmüller, P. G.; Bellei, M.; Battistuzzi, G.; Stadlmann, J.; Vlastis, J.; Obinger, C. *Biochem. J.* **2009**, *418*, 443−451.
(68) Zámocký, M.; Droghetti, E.; Bellei, M.; Gasselhuber, B.; Pabst, M.; Furtmüller, P. G.; Battistuzzi, G.; Smulevich, G.; Obinger, C. *Biochimie* **2012**, *94*, 673−683.
(69) Jensen, G. M.; Goodin, D. B. *Theor. Chem. Acc.* **2011**, *130*, 1185−1196.
(70) (a) Sligar, S. G. *Biochemistry.* **1976**, *15*, 5399−5406. (b) Sligar, S. G.; Gunsalus, I. C. *Proc. Natl. Acad. Sci. U.S.A.* **1976**, *73*, 1078−1082. (c) Fisher, M. T.; Sligar, S. G. *J. Am. Chem. Soc.* **1985**, *107*, 5018−5019. (d) Johnson, D. L.; Conley, A. J.; Martin, L. L. *J. Mol. Endocrinol.* **2006**, *36*, 349−359.
(71) (a) Guengerich, F. P. *Biochemistry* **1983**, *22*, 2811−2820. (b) Yamazaki, H.; Johnson, W. W.; Ueng, Y. F.; Shimada, T.; Guengerich, F. P. *J. Biol. Chem.* **1996**, *271*, 27438−27444. (c) Sligar, S. G.; Cinti, D. L.; Gibson, G. G.; Schenkman, J. B. *Biochem. Biophys. Res. Commun.* **1979**, *90*, 925−932.
(72) Segall, M. D.; Payne, M. C.; Ellis, S. W.; Tucker, G. T.; Eddershaw, P. J. *Xenobiotica* **1999**, *29*, 561−571.
(73) Das, A.; Grinkova, Y. V.; Sligar, S. G. *J. Am. Chem. Soc.* **2007**, *129*, 13778−13779.
(74) Rowland, P.; Blaney, F. E.; Smyth, M. G.; Jones, J. J.; Leydon, V. R.; Oxbrow, A. K.; Lewis, C. J.; Tennant, M. G.; Modi, S.; Eggleston, D. S.; et al. *J. Biol. Chem.* **2006**, *281*, 7614−7622.
(75) Alfonso-Prieto, M.; Biarmes, X.; Vidossich, P.; Rovira, C. *J. Am. Chem. Soc.* **2009**, *131*, 11751−11761.